Analytical & Numerical Modelings of Elliptical Superconducting Filament Magnetization

T. Satiramatekul, F. Bouillault, A. Devred and L. Bottura

Abstract—**This paper deals with the two-dimensional computation of magnetization in an elliptic superconducting filament by using numerical and analytical methods. The numerical results are obtained from the finite element method and by using Bean's model. This model is well adapted for Low T_c superconductor studies. We observe the effect of the axis ratio and of the field angle to the magnetic moment per unit length at saturation, and also to the cycle of magnetization. Moreover, the current density and the distribution of the electromagnetic fields in the superconducting filament are also studied.**

Index Terms—**Filament magnetization, Persistent currents, Current density distribution, Finite element method.**

I. Introduction

ONE of the major properties of superconductors is their absence of resistance when they are supplied by direct current. For this reason superconductors are commonly used to manufacture windings intended for the creation of high magnetic fields, as in the case of the electromagnets for the guidance of the beam in particle accelerators. However, when these materials are subjected to a variation of external magnetic field, they react so as to protect their bulk from the field variation. Shielding currents are generated at the periphery of the filament. In the absence of dissipative phenomena, the shielding currents are permanent, hence the name of *persistent currents*, and can degrade the quality of magnetic field produced by the magnet. In the case of particle accelerators, it is then necessary to envisage correction magnets whose design and powering is directly related to the amplitude of the persistent currents. The prediction of the persistent currents is usually based on analytical solutions valid only for circular filaments. In reality, however, the superconducting wires undergo large deformation during the manufacturing process, which leads to filament cross sections which do not have the theoretical shape of a circle. A first-order quantification of the influence of the shape of the filament on the electromagnetic behavior can be obtained by considering an elliptical section.

In this paper, we present the computation of magnetization of a superconducting, elliptical filament in two dimensions by using numerical and analytical methods. The cross-sectional area of the elliptical filament is assumed to be constant, equal to the cross-sectional area of a circular filament of 38 μm^2 (corresponding to a filament diameter of 7 μm as used for the LHC magnets at CERN). The finite element method (FEM) is used for the numerical calculation. This method allows to compute numerically the electromagnetic characteristic variables (penetration induction, magnetic moment per unit volume, etc.). These can also be obtained directly in some configurations if different integrals are performed analytically. The geometry considered is reported in Fig. 1. At first we have applied a magnetic field perpendicular to the x-axis (Fig. 1(b)), and then we have turned the applied field with an angle θ respect to the x-axis (Fig. 1(a)).

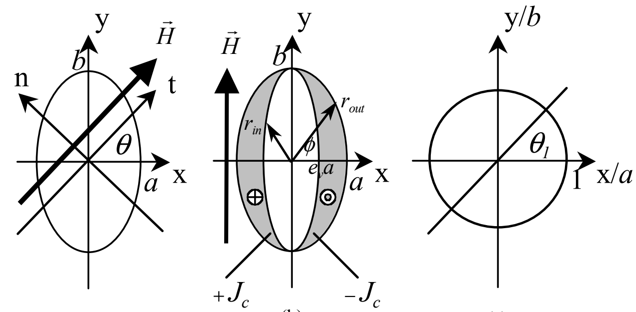

Fig. 1. (a) Elliptical cross section of superconducting filament submitted to an applied magnetic field *H(t)*, (b) Model of persistent magnetization current shell with elliptical inner boundary, and (c) Altering the reference axis from x, y axis to x/a, y/b axis (this change is used for solving the problem in the second case).

II. Problem Presentation

The electromagnetic behavior of superconducting devices can be described by Maxwell's equations, linking the electric field $\vec{e}$, the magnetic field $\vec{h}$, the magnetic induction $\vec{b}$ and the current density $\vec{j}$ [1]. With the elimination of magnetic variables, we have an equation which can be written in three dimensions as follows:

$$\frac{\partial \vec{j}}{\partial t} + \nabla \times \left(\frac{1}{\mu_0} \nabla \times \vec{e} \right) = \vec{0} \quad in \quad \Omega \qquad (1)$$

where μ_0 is the permeability of vacuum, Ω is the computational domain with boundary Γ.

In order to obtain a complete system, (1) must be complemented by a constitutive relation between $\vec{j}$ and $\vec{e}$. We have chosen to use the Bean's model [2], defined as:

T. Satiramatekul and F. Bouillault are with the Laboratoire de Génie Electrique de Paris (LGEP), CNRS UMR 8507, Supélec, Plateau de Moulon, 91192 Gif-sur-Yvette Cedex, France (e-mail: thitipong@lgep.supelec.fr).

A. Devred is with CEA, DSM/DAPNIA/SACM, 91191 Gif-Sur-Yvette Cedex, France, and CERN, AT-MAS, CH-1211, Geneva 23, Switzerland.

L. Bottura is with CERN, AT-MTM, CH-1211, Geneva 23, Switzerland.

$$\begin{cases} j < j_c & ; e = 0 \\ j = j_c & ; e \neq 0 \end{cases} \quad (2)$$

where $j = |\vec{j}|$, $e = |\vec{e}|$, $\vec{j} // \vec{e}$, and j_c is the critical current density. For numerical treatment, the functional dependence of $\vec{j}$ on $\vec{e}$ can be approximated by $j = \gamma(e)$ where γ is a nonlinear monotonic function discussed in [1].

III. Analytical Formulation

We consider an infinitely long, elliptical, superconducting filament with a major radius b and a minor radius a immersed in a uniform magnetic field $H(t)$ varying sinusoidally in time and forming an angle θ respect to the x-axis (see Fig. 1(a)). An analytical solution can be developed to obtain global magnetic quantities.

We consider initially the case of magnetic field applied parallel to the y-axis (θ = 90°), and limit ourselves to the analysis of the first field increase, for $0 \le t \le T/4$. The persistent currents flow in a shell at the filament periphery, and the inner boundary of the shell can be approximated by an ellipse [3] (Fig. 1(b)). The relation between the magnetic induction B ($B = \mu_0 H$) and eccentricity e_v of the elliptical inner boundary of the persistent current shell ($0 < e_v < 1$) is obtained by writing that the magnetic induction (or magnetic field) created by the persistent currents at the center of the filament is completely opposed to the source induction (or source field), that is to say:

$$B = \frac{2\mu_0 J_c}{\pi} \int_0^{\pi/2} \int_{r_{in}}^{r_{out}} d\rho \cos\phi \, d\phi \quad (3)$$

where r_{in} and r_{out} are defined in Fig. 1(b). After integration, we obtain the following relations:

$$B = \begin{cases} kB_0 \left(\frac{\sin^{-1}\sqrt{1-k^4}}{\sqrt{1-k^4}} - \frac{e_v \sin^{-1}\sqrt{1-e_v^2 k^4}}{\sqrt{1-e_v^2 k^4}} \right) & ; k < 1 \\ kB_0 \left(1 - \frac{e_v \sin^{-1}\sqrt{1-e_v^2}}{\sqrt{1-e_v^2}} \right) & ; k = 1 \\ kB_0 \left(\frac{\sinh^{-1}\sqrt{k^4-1}}{\sqrt{k^4-1}} - \frac{e_v \sin^{-1}\sqrt{1-e_v^2 k^4}}{\sqrt{1-e_v^2 k^4}} \right) & ; k > 1, e_v k^2 < 1 \\ kB_0 \left(\frac{\sinh^{-1}\sqrt{k^4-1}}{\sqrt{k^4-1}} - \frac{e_v \sinh^{-1}\sqrt{e_v^2 k^4 - 1}}{\sqrt{e_v^2 k^4 - 1}} \right) & ; k > 1, e_v k^2 > 1 \end{cases} \quad (4)$$

where $B_0 = 2\mu_0 J_c r / \pi$, $k^2 = a/b$ and we use an equivalent filament radius r defined as $\pi r^2 = \pi a b$. The cross-sectional area of the elliptical filament has been conserved for all calculations reported here, and has been taken equal to that of a typical LHC filament (7 μm diameter ($2 \times r$), 38 μm^2 cross section (πr^2)). Note that under this hypothesis r is a constant.

Total penetration of the filament by the shielding currents is reached when e_v = 0 in (4). The magnetic induction (or magnetic field) at which this occurs is the penetration induction B_p (or penetration field), found solving (4):

$$B_p = \begin{cases} \frac{kB_0}{\sqrt{1-k^4}} \tan^{-1}\sqrt{k^{-4}-1} & ; k < 1 \\ B_0 & ; k = 1 \\ \frac{kB_0}{\sqrt{k^4-1}} \tanh^{-1}\sqrt{1-k^{-4}} & ; k > 1 \end{cases} \quad (5)$$

An integration similar to (3) may be used to find the magnetic moment per unit volume:

$$M = -\frac{4\mu_0 J_c}{S} \int_0^{\pi/2} \int_{e_v}^{1} a^2 b u \, du \cos^3\phi \, d\phi \quad (6)$$

where S is the cross-sectional area of the elliptical filament, explicitly given by $S = \pi a b$. Finally, we obtain that:

$$M = \begin{cases} -\frac{2kB_0}{3}\left(1 - e_v^2\right) & ; B \le B_p \\ -\frac{2kB_0}{3} = M_s & ; B \ge B_p \end{cases} \quad (7)$$

where M_s is the magnetic moment per unit volume at saturation.

Equations (4), (5) and (7) hold for $0 \le t \le T/4$, where T is the period of the magnetic induction. For any time $t \ge T/4$ we can obtain the corresponding results by using the superposition of several states.

The calculation of a complete magnetization cycle requires the evaluation of e_v as a function of B by solving (4). We have fitted the solution of this implicit equation by a fourth order polynomial:

$$e_v = \alpha_4 \left(\frac{B}{B_p}\right)^4 + \alpha_3 \left(\frac{B}{B_p}\right)^3 + \alpha_2 \left(\frac{B}{B_p}\right)^2 + \alpha_1 \left(\frac{B}{B_p}\right) + \alpha_0 \quad (8)$$

where the coefficients α_0, α_1, α_2, α_3 and α_4 are a function of the ratio a/b. To obtain a practical expression, these coefficients have also been fitted by a polynomial in a/b.

The second case we consider is when the external field forms an angle θ respect to the x-axis, where $0° \le \theta \le 90°$. In this case we could only calculate the penetration induction and the magnetic moment per unit volume at saturation, due to the complexity of the problem. For more details we resort to numerical techniques. Referring to Fig. 1, using the geometries in Fig. 1(a) and 1(c), we may write that:

$$B_p = B_1 \left(\int_0^{\cos\theta_1} \frac{b\cos\theta \, du}{b^2 + (a^2 - b^2)u^2} + \int_0^{\sin\theta_1} \frac{a\sin\theta \, du}{a^2 + (b^2 - a^2)u^2} \right) \quad (9)$$

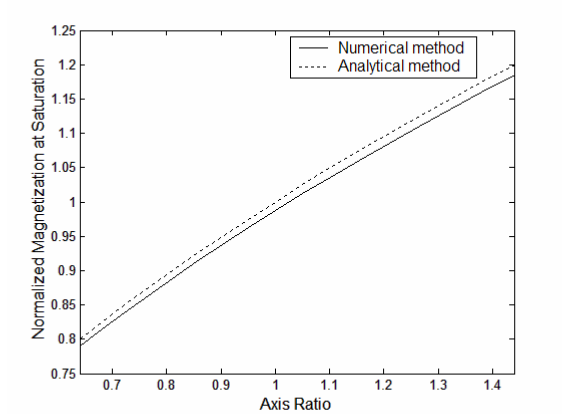

Fig. 2. Comparison between the normalized magnetic moment per unit volume at saturation $M_s/M_{s,cylinder}$ where $M_{s,cylinder} = M_s$ at $a = b$ (or $k = 1$) versus the axis ratio a/b obtained from the numerical method and that obtained from the analytical method.

where $B_1 = 2\mu_0 J_c ab/\pi$ and $\theta_1 = \tan^{-1}(k^2 \tan\theta)$.
Integrating (9) we find:

$$B_p = \begin{cases} \dfrac{kB_0}{\sqrt{1-k^4}}\left[\begin{array}{l}\cos\theta\tanh^{-1}\left(\cos\theta_1\sqrt{1-k^4}\right)\\ +\sin\theta\tan^{-1}\left(\sin\theta_1\sqrt{k^{-4}-1}\right)\end{array}\right] & ;k<1 \\ \dfrac{B_0}{k}\left[k^2\cos\theta\cos\theta_1+\sin\theta\sin\theta_1\right] & ;k=1 \\ \dfrac{kB_0}{\sqrt{k^4-1}}\left[\begin{array}{l}\cos\theta\tan^{-1}\left(\cos\theta_1\sqrt{k^4-1}\right)\\ +\sin\theta\tanh^{-1}\left(\sin\theta_1\sqrt{1-k^{-4}}\right)\end{array}\right] & ;k>1 \end{cases} \quad (10)$$

The magnetic moments per unit volume at saturation, in the directions perpendicular and parallel to the applied magnetic field, are given by the following expressions:

$$M_{n,s} = -M_{x,s}\sin\theta + M_{y,s}\cos\theta \quad (11)$$

$$M_{t,s} = M_{x,s}\cos\theta + M_{y,s}\sin\theta \quad (12)$$

where $M_{x,s} = -\dfrac{2B_0}{3k}\cos\theta_1$, $M_{y,s} = -\dfrac{2kB_0}{3}\sin\theta_1$.
Substituting these relations in (11) and (12) we come to the following result:

$$M_{n,s} = -\frac{2B_0}{3k}\left[k^2\sin\theta_1\cos\theta - \cos\theta_1\sin\theta\right] \quad (13)$$

$$M_{t,s} = -\frac{2B_0}{3k}\left[k^2\sin\theta_1\sin\theta + \cos\theta_1\cos\theta\right] \quad (14)$$

IV. Numerical Formulation

A numerical solution of (1) can be obtained by using the finite element method. After integration, the weak formulation of our problem is summarized in the following statement:

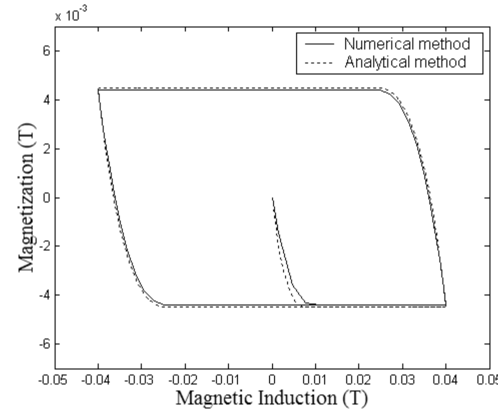

Fig. 3. Comparison of the cycles of magnetization obtained by using the numerical and analytical methods, where $a/b = 0.64$.

For $h(t)$ given, at any time $t \geq 0$, find e in $H^1(\Omega)$ such that $e = 0$ at $t = 0$ and

$$\int_\Omega \frac{\partial\gamma(e)}{\partial t} e'dx + \int_\Omega \mu_0^{-1}\nabla e\cdot\nabla e'dx - \int_\Gamma \frac{\partial h_{tg}}{\partial t} e'd\Gamma = 0\,;\forall e'\in H^1(\Omega) \quad (15)$$

where e' is the test function which is equal to the shape function φ used to interpolate e (Galerkin's method), and $H^1(\Omega)$ is the Sobolev's space.

Discretizing in space we obtain an algebraic system which can be written in the following matrix form:

$$[M]\frac{\partial J}{\partial t} + [A]E = F \quad (16)$$

where E and J which depend on time are the vectors of degrees of freedom of the electric field and of the current density respectively. More details can be found in [4].

V. Analytical and Numerical Results

We have carried out a first series of simulations for a superconducting filament with an elliptical cross section ($0.64 \leq a/b \leq 1.44$) immersed in a uniform magnetic field which is parallel to the y-axis ($\theta = 90°$) and varying sinusoidally in time $h_y(t) = h\sin(2\pi f t)$ at 50 Hz. The critical current density J_c is taken equal to 3×10^9 A/m^2. Fig. 2 illustrates the influence of the shape of the ellipse on the magnetic moment per unit volume at saturation. The analytical and numerical results are in very good agreement, the difference between two curves is only 1.3 %. In practice, a deformation of the filament can lead to a significant variation of the magnetization, i.e. 20 % in the modest range of aspect ratio explored. Fig. 3 shows the difference between the cycles of magnetization calculated numerically and analytically. We observe that the curves are nearly identical.

In a second series of simulations, we have considered an elliptical superconducting filament plunged in a sinusoidal magnetic field whose field angle is equal to θ compared with the x-axis, where $0° \leq \theta \leq 90°$. In Figs. 4 and 5 we study the influence of the axis ratio and the field angle on the magnetic

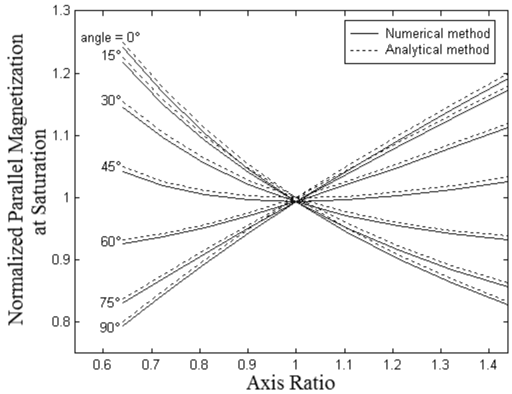

Fig. 4. Normalized magnetic moment per unit volume at saturation, parallel to the applied magnetic field, $M_{t,s}/M_{s,cylinder}$ as a function of axis ratio a/b obtained from the numerical and analytical methods for the different field angles θ.

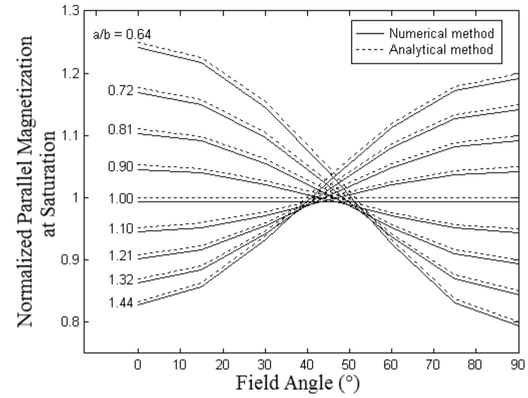

Fig. 5. Normalized magnetic moment per unit volume at saturation, parallel to the applied magnetic field, $M_{t,s}/M_{s,cylinder}$ as a function of field angle θ obtained from the numerical and analytical methods for the different axis ratios a/b.

moment per unit volume at saturation. We find that the functional dependence of the normalized magnetic moment per unit volume at saturation on the aspect ratio (Fig. 4) and the field angle (Fig. 5) is almost identical in both computations (numerical and analytical). From Figs. 4 and 5 we see that the magnetization depends both on the axis ratio a/b and the field angle θ. If we take in particular Fig. 4, the tendency of $M_{t,s}/M_{s,cylinder}$ for $a/b < 1$ is to decrease at increasing θ, with minimum magnetization at $\theta = 90°$. This corresponds to the case of a thin filament, oriented vertically and with field along the y axis. The variation of the magnetization with a change of angle is reversed at $a/b < 1$, and, as expected, a flat filament, oriented horizontally, has minimum magnetization when the field is applied along the x-axis. Finally, the dependence on the angle is stronger at larger aspect ratio.

With the numerical method, we could obtain the cycles of magnetization (see Fig. 6). We observe that, except for $\theta = 0°$ and $\theta = 90°$, the magnetic moment is not co-linear with the applied magnetic induction. These results are in agreement with (13) and (14).

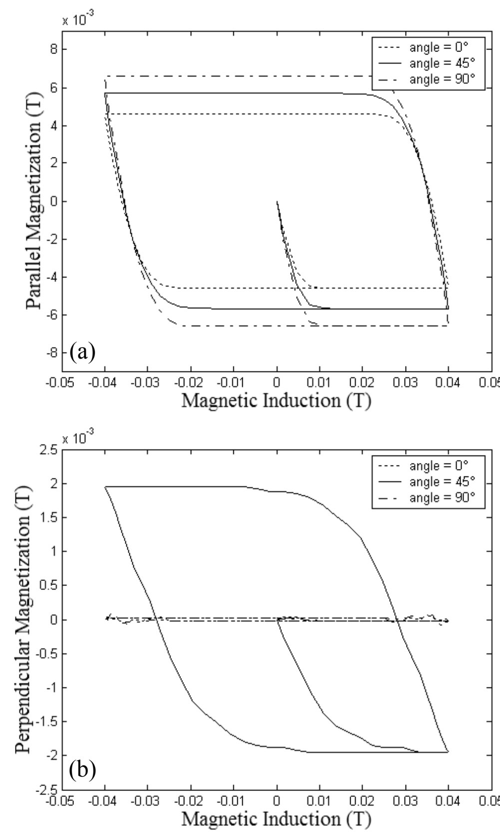

Fig. 6. Cycles of magnetization, (a) parallel and (b) perpendicular to the applied magnetic field, obtained from the numerical method for the different field angles θ, where $a/b = 1.44$.

VI. Conclusion

Analytical formulae in 2D have been developed for an elliptical superconducting filament. The analytical formulae have been validated by comparison to numerical results obtained using a code based on finite elements and Bean's constitutive law. Using these formulations, we could calculate the magnetization and obtain the cycle of magnetization in cases relevant to the strand used for the LHC magnets. We have studied the influence of the aspect ratio of the ellipse and the field angle on the magnetization and found variations of the order of 20 % in the range of expected deformations of the round filaments.

Acknowledgements

We gratefully acknowledge the support and contribution of D. Leroy and R. Wolf (CERN) who have actively participated in the discussion of the ideas presented in this paper.

References

[1] M. Maslouh, F. Bouillault, A. Bossavit, and J. C. Verite, "From Bean's model to the H-M characteristic of a superconductor: some numerical experiments," *IEEE Trans. Magn.*, vol. 7, no. 3, pp. 3797–3800, 1997.

[2] C. P. Bean, "Magnetization of hard superconductors," *Phys. Rev. Lett.*, vol. 8, pp. 250–253, 1962.

[3] M. N. Wilson, *Superconducting magnets*. Oxford: Oxford University Press, 1983, pp. 165–166.

[4] M. Maslouh, F. Bouillault, and J. C. Verite, "Two-dimensional numerical modeling of superconductors with imposed currents by the finite element method," *IEEE Trans. Magn.*, vol. 36, no. 4, pp. 1234–1237, 2000.